

AN ADAPTIVE SHRINKAGE FUNCTION FOR IMAGE DENOISING BASED ON NEIGHBORHOOD CHARACTERISTICS

YING YANG^{✉,1} AND YUSEN WEI^{1,2}

¹Xi An University of Technology, Dept. of EE, Xi An, China, 710048; ²Xi An Vocational University of Automobile, Xi An, 710600 China.

e-mail: yangy@xaut.edu.cn; wyshyy@aliyun.com

(Received March 24, 2021; accepted June 29, 2022)

ABSTRACT

The shrinkage function has an important effect on the image denoising results. An adaptive shrinkage function is developed in this paper to shrink the small coefficients properly for image denoising based on neighborhood characteristics. The shrinkage function is determined by the number of large coefficients near the current signal coefficients. In this way, different shrinkage functions can be adaptively used to deal with different coefficients in the process of image denoising, instead of using fixed shrinkage functions. Experimental results show that the SNR of the image processed by the adaptive shrink function algorithm is better than that processed by the soft threshold, hard threshold, and neighborhood shrink algorithm. Moreover, compared with the traditional soft threshold, hard threshold and neighborhood shrink algorithm, the PSNR of the algorithm using adaptive shrink function increases by 3.68dB, 2.28dB and 0.61dB, respectively. In addition, the proposed new algorithms, soft threshold and hard threshold, are combined with empirical Wiener filtering and shift invariant (TI) scheme to compare their image noise reduction effects. The results show that the PSNR can be improved significantly by using the adaptive shrink function algorithm combined with empirical Wiener filtering and shift invariant (TI) scheme.

Keywords: image denoising, neighboring coefficients, wavelet transforms.

INTRODUCTION

Noise suppression without losing too much image information is a complicated problem in the image processing. The wavelet transform has become a favorable technique that removes noise from the noisy contaminated images in many different areas, such as hyperspectral image denoising (Alessandro *et al.*, 2020), feature extraction (Lalith *et al.*, 2021 and Çelik *et al.*, 2008), face recognition (Fadi *et al.*, 2022 and Yu-Hsuan *et al.*, 2022), etc. The basic steps of the image denoising include firstly, transforming the noisy image into a wavelet domain by the two-dimensional (2D) discrete wavelet transform; secondly, thresholding the wavelet coefficients in the wavelet domain and finally, performing the inverse 2D wavelet transform to obtain the denoised image. Both the soft and hard thresholding method (Dohono, 1995; Dohono *et al.*, 1994 and Dohono *et al.*, 1995) are also frequently used because of their effectiveness and simplicity. However, there are some disadvantages to these two methods. For example, a bigger bias would occur when the soft thresholding shrunk the large coefficients. Due to the discontinuities of the shrinkage function, the hard thresholding algorithm exhibited visual artifacts (Gibbs phenomena) in the neighborhood of discontinuities

(Coifman *et al.*, 1995). To overcome the drawbacks of soft and hard thresholding, a lot of methods have been proposed. Such as, the TI scheme (Coifman *et al.*, 1995), the random interpolation average scheme (Ying *et al.*, 2010 and Ying *et al.*, 2013), the empirical wiener filtering (Choi *et al.*, 1998; Ghael *et al.*, 1997 and Choi *et al.*, 2004), and the *NeighShrink* scheme (Chen *et al.*, 2003 and Cai *et al.*, 2001)

Many algorithms have emerged on the image denoising using the improved techniques to improve the denoised capability. The spatially adaptive wavelet thresholding method based on a context modeling was proposed in (Chang *et al.*, 2000). This work applied the context modeling to estimate the parameter for each coefficient, which was then used to adapt the thresholding strategy. In ref. (Shengqian *et al.*, 2002), the shrinkage thresholds were calculated according to the neighborhood characteristics and the noise level. The adaptive thresholding algorithm resulted in an efficient method for the image denoising. In ref. (Chen *et al.*, 2005) an efficient adaptive algorithm was proposed. The adaptive threshold was applied to capture the dependency of inter-scale wavelet coefficients. In ref. (Sendur *et al.*, 2002a and Sendur *et al.*, 2002b), a nonlinear bivariate shrinkage function

was proposed for the image denoising. Their method was based on the new non-Gaussian bivariate distributions to model the inter-scale dependencies. Simoncelli and Adelson (Simoncelli *et al.*, 1996) developed a Bayesian estimator that provided a natural extension for incorporating the higher-order statistical regularity presented in the point statistics of subband representation. The customized *NeighShrink* (Chen *et al.*, 2005) applied the customized wavelet to replace the fixed wavelet in the *NeighShrink* denoising. The numerical results showed that it was better than the *NeighShrink* scheme obviously. In ref. (Zhou *et al.*, 2008), the authors improved the *NeighShrink* scheme using the Stein's unbiased risk estimate. It could estimate an optimal threshold and the neighboring window size for the *NeighShrink* scheme in every wavelet subband. The experimental results demonstrated that it outperformed the *NeighShrink* scheme.

Traditional denoising methods set small coefficients to zero or shrink them using a fixed shrinkage function. The values of a small coefficient are often less than or equal to the threshold, so that they are filtered by the threshold. However, in fact, some of the small coefficients contain a lot of useful information about the image. If these kinds of coefficients can be preserved or shrunk properly, it is no doubt that better results will be given. An adaptive shrinkage function algorithm for image denoising is proposed in this paper. In this algorithm, the coefficients with values larger than the threshold will be kept originally. Each small coefficient would be properly shrunk by a special shrinkage function. According to the number of the large coefficients in the neighborhood of the current small coefficient, the shrinkage function was determined. Because different small coefficients are thresholded using different shrinkage functions in our method, more image features will be preserved.

MATERIAL AND METHODS

WAVELET TRANSFORMS AND IMAGE DENOISING

In 2D wavelet transforms (Gonzalez *et al.*, 2002 and Mallat *et al.*, 1989), one 2D scaling function ($\varphi(x,y)$) and three 2D wavelets ($\psi^H(x,y)$, $\psi^V(x,y)$ and $\psi^D(x,y)$) are required. They are the product of the one-dimensional scaling function $\varphi_{j,k}(t)=2^{-j/2}\varphi(2^{-j}t-k)$ and the corresponding wavelet $\psi_{j,k}(t)=2^{-j/2}\psi(2^{-j}t-k)$ and can be expressed as $\varphi(x,y)=\varphi(x)\varphi(y)$, $\psi^H(x,y)=\psi(x)\varphi(y)$, $\psi^V(x,y)=\varphi(x)\psi(y)$ and $\psi^D(x,y)=\psi(x)\psi(y)$, respectively.

The discrete wavelet transform of the image $I(x,y)$ with a size of $M \times N$ is satisfied by the equation (1) and (2)

$$W_\varphi(J,m,n) = \frac{1}{\sqrt{MN}} \sum_{x=0}^{M-1} \sum_{y=0}^{N-1} I(x,y) \varphi_{J,m,n}(x,y) \quad (1)$$

$$W_\psi^i(j,m,n) = \frac{1}{\sqrt{MN}} \sum_{x=0}^{M-1} \sum_{y=0}^{N-1} I(x,y) \psi_{j,m,n}^i(x,y) \quad i = \{H, V, D\} \quad (2)$$

Where, the index i identifies the directional wavelets in equation (2), J is the largest (or coarsest) scale in the decomposition, $W_\varphi(J,m,n)$ is the approximate coefficients of $I(x,y)$ at the scale J . $W_\psi^i(j,m,n)$ is the detail coefficients along different directions at the scale $j(j=1,2,\dots,J)$.

The 2D orthogonal wavelet transform of images is shown in Fig. 1. The decomposition and reconstruction subbands are listed at the top and the bottom rows in Fig. 1. The wavelet coefficients are arranged as the independent square matrices during image denoising. Four frequency subbands (A , DH , DV , and DD) are produced by each decomposition step. The wavelet transform could be done recursively through decomposing the low frequency wavelet coefficients (subband A_j) which are produced by the previous decomposition step.

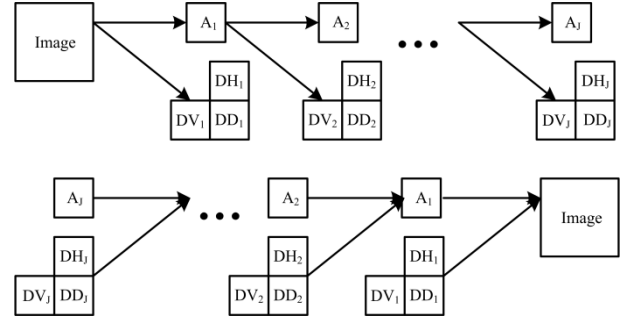


Fig. 1. *Subbands of 2D orthogonal wavelet transform.*

Because most of the Gaussian white noise can be averaged out in low frequency wavelet coefficients, the small coefficients in subband A_j are mainly contributed from the image and should be kept. Only high frequency wavelet coefficients (subbands DH , DV , and DD) should be thresholded. Only in this way can the denoised image retain more information about the original image and be as close as possible to the original image. The reconstruction of denoised image is obtained by the inverse discrete wavelet transform

$$\hat{I}(x, y) = \frac{1}{\sqrt{MN}} \sum_m \sum_n W_\varphi(J, m, n) \varphi_{J, m, n}(x, y) + \frac{1}{\sqrt{MN}} \sum_{i=H, V, D} \sum_{j=1}^J \sum_m \sum_n \hat{W}_\psi^i(j_0, m, n) \psi_{j, m, n}^i(x, y) \quad (3)$$

The shrinkage functions of soft and hard thresholding can be expressed as

$$\hat{W}_{j,k} = \begin{cases} 0, & |W_{j,k}| \leq T \\ \text{sgn}(W_{j,k})(|W_{j,k}| - T), & |W_{j,k}| > T \end{cases} \quad (4)$$

$$\hat{W}_{j,k} = \begin{cases} 0, & |W_{j,k}| \leq T \\ W_{j,k}, & |W_{j,k}| > T \end{cases} \quad (5)$$

where, T ($T = \sigma \sqrt{2 \log(MN)}$) is the universal threshold, σ^2 is the noise variance, $M \times N$ is the number of pixels. If the noise variance is unknown, it can be estimated in the subband DD_1 by a robust median estimator (Dohono *et al.*, 1994).

$$\sigma = \frac{\text{Median}(|y_{j,k}|)}{0.6745}, \quad y_{j,k} \in \text{subband } DD_1 \quad (6)$$

The universal threshold will be used in all the denoising methods in our experiments.

ADAPTIVE SHRINKAGE FUNCTIONS ALGORITHM DESCRIPTION

Neighboring coefficients with similar information are guaranteed by the convolution of the image $I(x,y)$ with the wavelet basis. The distance between two coefficients and the wavelet basis will decide how similar they are. The closer the distance of two coefficients, the more similar they are. Generally, small coefficients are set to zero because they are from the noise. Large coefficients are kept or shrunk by a thresholding policy because they are contributed by the image. As far as the similarity of two neighboring coefficients is concerned, it is impossible that the small coefficient is completely from the noise signal, while the large coefficient is completely from the image. According to analysis, if the small coefficient is neighbored with one or more large coefficients, it should be filtered by a special shrinkage function rather than setting it to zero. It is beneficial for preserving the image information. The following shrinkage functions are proposed for the image denoising.

$$\hat{W}_{j,k} = \begin{cases} W_{j,k} & |W_{j,k}| > T \\ W_{j,k} \cdot (1 - (T / (|W_{j,k}| + T))^r) & |W_{j,k}| \leq T \end{cases} \quad (7)$$

where, r is the number of the large coefficients in the neighborhood. For image denoising, wavelet coefficients $W_{j,k}^i(j, m, n)$ are filtered one by one using different shrinkage functions, on the basis of their individual r values. The denoised image is reconstructed by taking the thresholded coefficients $\hat{W}_{j,k}^i(j, m, n)$ into the equation (3). The input-output characteristics of the proposed shrinkage functions for different r values are shown in Fig. 2.

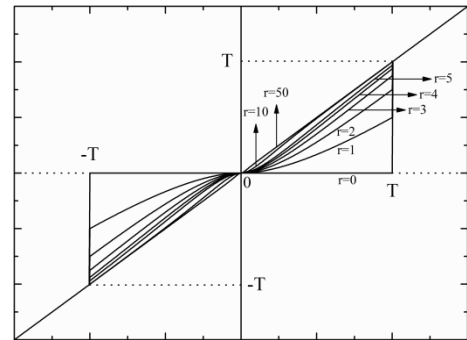


Fig. 2. The input-output characteristics of the proposed shrinkage functions.

According to equation (7), large coefficients are kept. The difference between the proposed method and the other methods is the shrinkage of the small coefficients. In order to properly shrink the small coefficients, the adaptive shrinkage functions are employed. The small coefficient with no neighboring large coefficient ($r=0$) is set to zero. In this case, the proposed method and the hard thresholding were the same. If $r > 0$, small coefficients are shrunk by different shrinkage functions determined by different r values. Note that the larger the r , the larger the thresholded coefficient is. Because the characteristics of neighboring coefficients are considered, the proposed method should have better denoising results. It can be reflected by the comparison of the mean square error (MSE). The MSE (risk) is defined as equation (8).

$$MSE = \frac{1}{M \cdot N} \sum_{x=1}^M \sum_{y=1}^N (I(x, y) - \hat{I}(x, y))^2 \quad (8)$$

where, $I(x,y)$ is the noise-free image and $\hat{I}(x,y)$ is the denoised image. We assumed that Tr represents the 2D wavelet transform and Tr^{-1} represents the inverse 2D wavelet transform, then the MSE is expressed as equation (9).

$$MSE = \frac{1}{M \cdot N} \sum_{x=1}^M \sum_{y=1}^N (Tr^{-1}(Tr(I(x, y))) - Tr^{-1}(Tr(\hat{I}(x, y))))^2 \quad (9)$$

Note that the transform preserves the vector lengths when Tr and Tr^{-1} are orthogonal. Thus, the MSE satisfies equation (10).

$$MSE = \frac{1}{M \cdot N} \sum_{x=1}^M \sum_{y=1}^N (Tr(I(x, y)) - Tr(\hat{I}(x, y)))^2 \quad (10)$$

where, $Tr(I(x, y))$ represents the wavelet coefficients of the noise-free image, $Tr(\hat{I}(x, y))$ denotes the wavelet coefficients of the denoised image. Equation (10) can be rewritten as equation (11).

$$MSE = \frac{1}{M \cdot N} \sum (a^o - a)^2 + \frac{1}{M \cdot N} \sum (W^o - \hat{W})^2 \quad (11)$$

where, a^o is approximation coefficients of the noise-free image, a is approximation coefficients of the noisy image, W^o is detail coefficients of the original image and \hat{W} is thresholded detail coefficients of the noisy image. Because the approximate coefficients are kept during the image denoising, the first item on the right side of equation (11) can be neglected. Both W^o and \hat{W} can be divided into three parts

$$W^o = W_{>T}^o + W_{r=0}^o + W_{r>0}^o \quad (12)$$

$$\hat{W} = \hat{W}_{>T} + \hat{W}_{r=0} + \hat{W}_{r>0} \quad (13)$$

where, $W_{>T}^o$ and $\hat{W}_{>T}$ represent those coefficients larger than the threshold, $W_{r=0}^o$ and $\hat{W}_{r=0}$ denote small coefficients with no neighbored large coefficients ($r=0$), $W_{r>0}^o$ and $\hat{W}_{r>0}$ denote small coefficients neighbored with one or more large coefficients ($r>0$).

The thresholded coefficients resulted from other methods and the proposed method are same except for the third part ($\hat{W}_{r>0}$). The third part resulted from other methods and the proposed method can be represented by $\hat{W}_{r>0}^H$ and $\hat{W}_{r>0}^P$, respectively. In other image denoising methods, due to fixed shrink function, many small coefficients are directly filtered whether they contained the useful information or not. However, in the adaptive shrink function method, the value of $\sum (W_{r>0}^o - \hat{W}_{r>0}^P)^2$ and $\sum (W_{r>0}^o - \hat{W}_{r>0}^H)^2$ still should be compared before the small coefficients are killed. Thus, the small coefficients are set to zero until the value of $\sum (W_{r>0}^o - \hat{W}_{r>0}^P)^2$ is less than that of $\sum (W_{r>0}^o - \hat{W}_{r>0}^H)^2$. It means that the small coefficients neighbored with one or more large coefficients will be shrunk properly rather than setting to zero. Therefore, Useful image information carried by small coefficients is preserved in the detail wavelet coefficients. For example,

supposing W_n^P is an arbitrary coefficient of $\hat{W}_{r>0}^P$, and W_n^H and W_n^o are the corresponding coefficients of $W_{r>0}^H$ and $W_{r>0}^o$. Then, when equation (14) holds, the method employing adaptive shrink function gives a lower risk.

$$(W_n^o - \hat{W}_n^P)^2 < (W_n^o - \hat{W}_n^H)^2 \quad (14)$$

Note that $W_{r>0}^H$ is set to zero and $\hat{W}_n^P = W_n^P \cdot (1 - (T / (|W_n^P| + T))^r)$. Then equation (14) can be expressed as equation (15)

$$(W_n^o - d \cdot W_n^P)^2 < W_n^{o2} \quad (15)$$

where, d ($d = 1 - (T / (|W_n^P| + T))^r$) is an attenuation coefficient. Obviously, $0 < d < 1$. It is easy to get equation (16)

$$|d \cdot W_n^P| < |2 \cdot W_n^o| \quad (16)$$

where, W_n^o can be treated as the original components of W_n^P . If the relationship between W_n^o and W_n^P satisfied equation (16), our method would give a lower risk than the other denoising methods.

The proposed method for image denoising can be concluded as follows

- 1) Perform the 2D wavelet transform on the noisy image to get the wavelet coefficients.
- 2) Apply the proposed method to shrink the wavelet coefficients.
 - a) Keep the large coefficients;
 - b) Count the value r of each small coefficient in an $n \times n$ neighborhood window;
 - c) Shrink the small coefficients using different shrinkage functions determined by different values of r .
- 3) Perform the inverse 2D wavelet transform on thresholded wavelet coefficients to get the denoised image.

NEIGHBORHOOD WINDOW SIZE OPTIMIZATION

The value r of every small coefficient $W_{j,k}$ needs to be counted so as to determine the shrinkage function which is used to shrink the small coefficient itself. A square window $B_{j,k}$ of $n \times n$ centered at $W_{j,k}$ is considered. Where, n is an odd number. A small coefficient and its neighborhood windows (3×3 and 9×9) are illustrated in Fig. 3. The size of $B_{j,k}$ determined the value r and the denoising efficiency.

Thus, the comparison experiments are performed to select an optimal size of $B_{j,k}$. Different wavelet coefficient subbands are independently thresholded in the proposed method. In the boundary regions of each subband (the pixel indices of $B_{j,k}$ is out of the wavelet subband range), the coefficients are thresholded using the hard thresholding. The images used in the experiments are the 512×512 and 256×256 gray level standard images of Lena, Cameraman, Barbara and Peppers. The original images are shown in Fig. 4. The noisy images are obtained by adding the zero mean white Gaussian noise with a standard variance σ_n ($\sigma_n = 25$) to the original images. Different neighborhood window sizes are used in the experiments. The symmlet wavelet with eight vanishing moments (sym8) and the decomposition level up to 3 are employed in the wavelet transform. The denoised results in Peak Signal to Noise Ratio (PSNR) are listed in Table 1. The PSNR is defined as equation (17)

$$PSNR = 10 \log_{10} \left(\frac{255^2 M}{\sum (I(i, j) - \hat{I}(i, j))^2} \right) \quad (17)$$

Generally, with the size of the window increased, the number of involved neighboring coefficients increased, and the r -value becomes large. However, the large window size will result in the large boundary regions which needs to be thresholded by hard thresholding. That is to say, different size of the neighborhood window will lead to different denoising capabilities. According to Table 1, the neighborhood window sizes of 9×9 , 11×11 and 13×13 are good choices. Especially for the size of 11×11 , it provides the best results and is employed in our method.

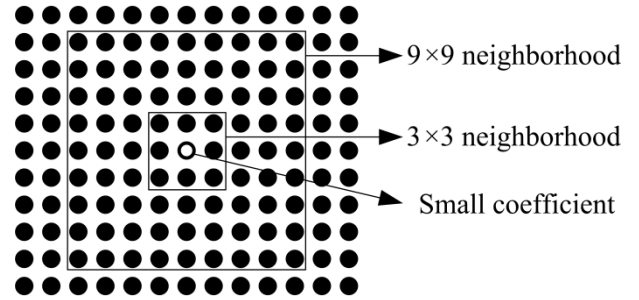


Fig. 3. The illustration of a small coefficient and its neighborhood windows.

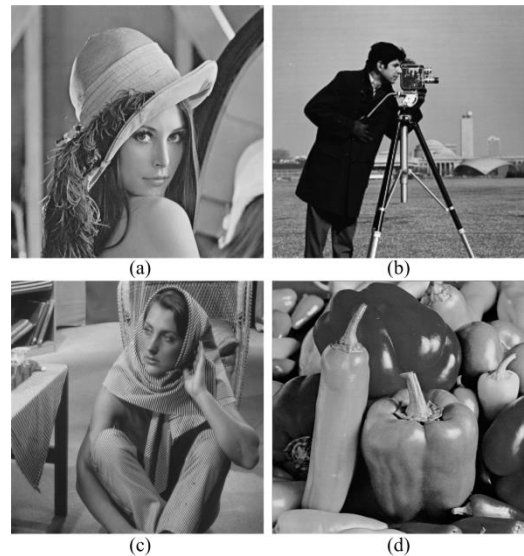


Fig. 4. Original images: (a) Lena, (b) Cameraman, (c) Barbara, (d) Peppers.

Table 1. Denoised results (dB) of the proposed method with different window sizes.

Image size (pixel)	PSNR _{in} (dB)	Window size (pixel)							
		1x1	3x3	5x5	7x7	9x9	11x11	13x13	15x15
Lena									
512x512	20.24	27.49	28.33	28.87	29.20	29.36	29.41	29.43	29.31
256x256	20.25	24.60	25.45	25.98	26.37	26.56	26.64	26.66	26.30
Cameraman									
512x512	20.56	27.58	28.73	29.32	29.64	29.82	29.86	29.86	29.64
256x256	20.53	23.94	25.06	25.70	25.99	26.14	26.20	26.18	26.15
Barbara									
512x512	20.24	23.69	24.39	25.02	25.50	25.84	26.07	26.22	26.17
256x256	20.25	24.41	25.02	25.43	25.67	25.85	25.96	26.03	25.63
Peppers									
512x512	20.44	27.24	28.11	28.56	28.75	28.81	28.65	28.52	28.15
256x256	20.34	25.31	26.35	26.94	27.19	27.33	27.37	27.23	26.47
Average	20.36	25.53	26.43	26.98	27.29	27.46	27.52	27.51	27.23

EXPERIMENTAL COMPARISON

The adaptive shrink function method, soft thresholding, hard thresholding, and *NeighShrink* method are applied to denoise the same group of images to compare the denoising effect. The zero mean Gaussian white noise with different noise levels ($\sigma=10, 15, 20, 25, 30$) are added to the noise-free images (Fig. 4) to obtain the noisy images. The ‘sym8’ wavelet and the decomposition level up to 3 are also employed in the wavelet transform.

RESULTS AND DISSCUSION

DIRECT COMPARISONS

The PSNR values of noisy images are depended on noise variances. The denoised images (noise level $\sigma=20$) and their zoomed local regions provided by four methods are illustrated in Fig. 5, 6, 7, and 8, respectively. The denoised results in PSNR are listed in Table 2.

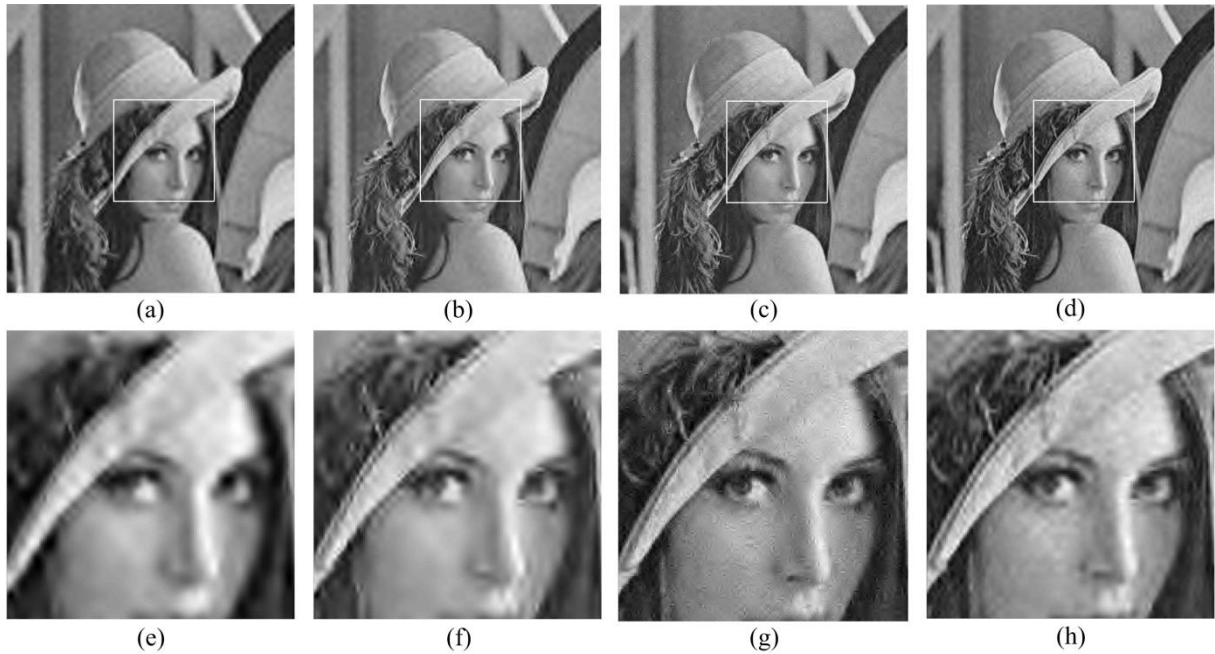


Fig. 5. The comparison of four methods on the 512×512 Lena with $\sigma=20$. (a) soft thresholding (27.10dB), (b) hard thresholding (28.30dB), (c) neighshrink (29.11dB), (d) our method (30.38dB); (e), (f), (g), (h) are the zoomed local regions of (a), (b), (c), (d), respectively.

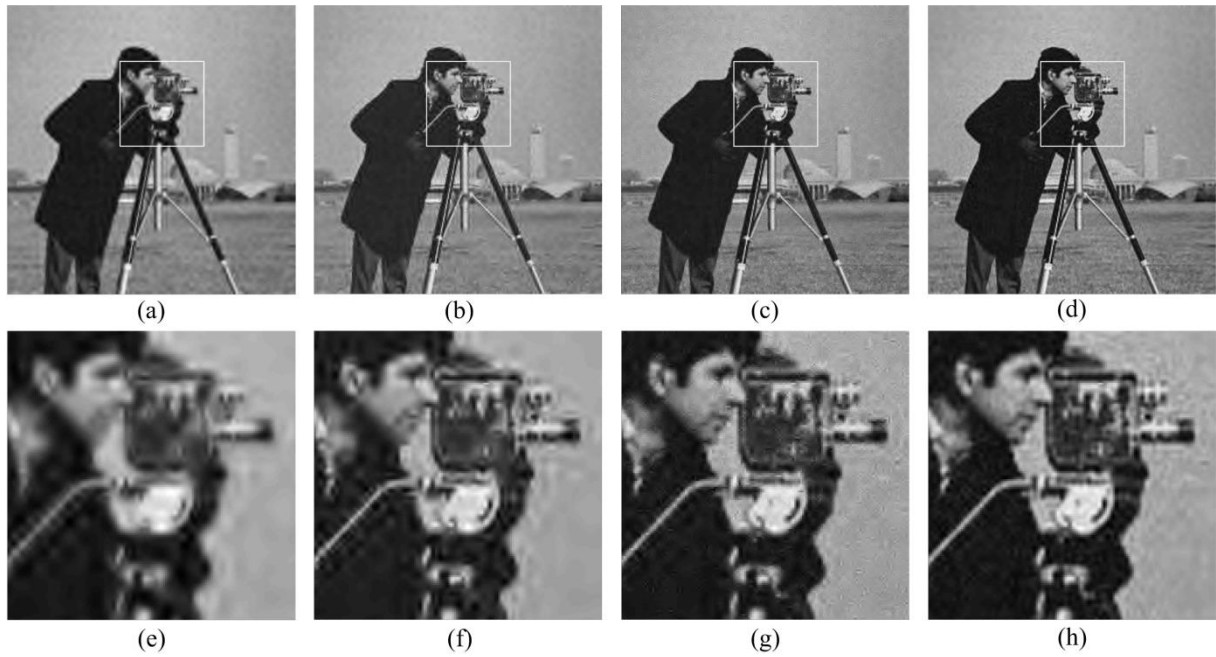


Fig. 6. The comparison of four methods on the 512×512 Cameraman with $\sigma=20$. (a) soft thresholding (26.84dB), (b) hard thresholding (28.73dB), (c) neighshrink (29.31dB), (d)our method (31.22dB); (e), (f), (g), (h) are the zoomed local regions of (a), (b), (c), (d), respectively.

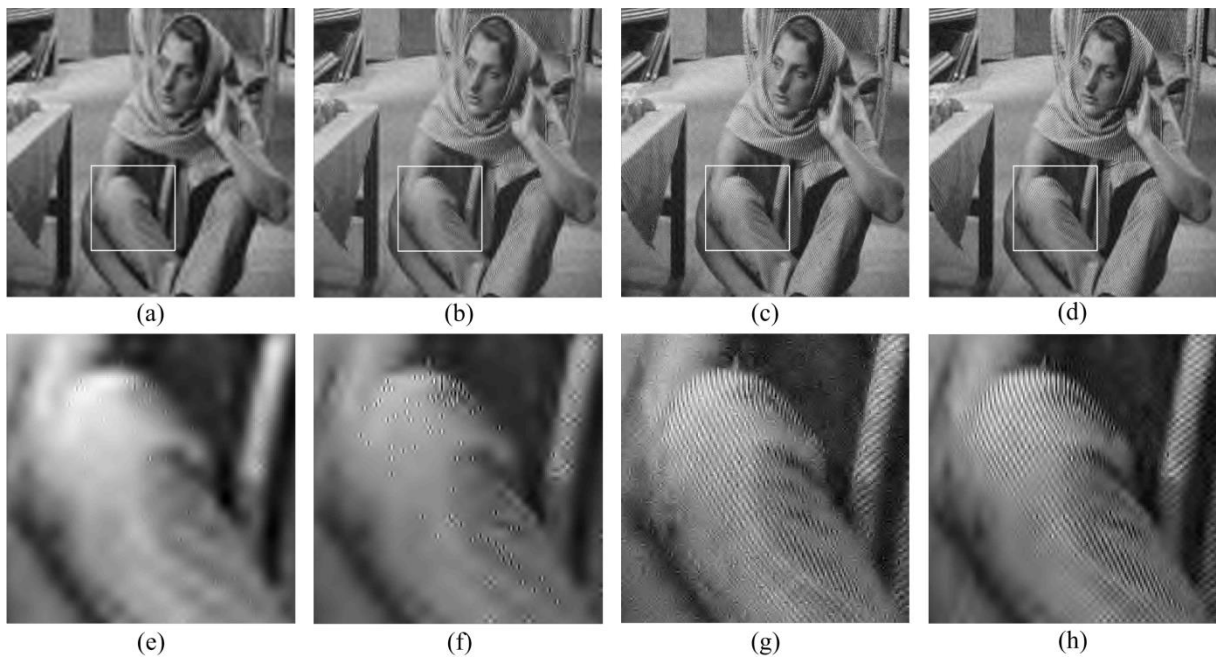


Fig. 7. The comparison of four methods on the 512×512 Barbara with $\sigma=20$. (a) soft thresholding (23.45dB), (b) hard thresholding (24.32dB), (c) neighshrink (27.22dB), (d)our method (27.39dB); (e), (f), (g), (h) are the zoomed local regions of (a), (b), (c), (d), respectively.

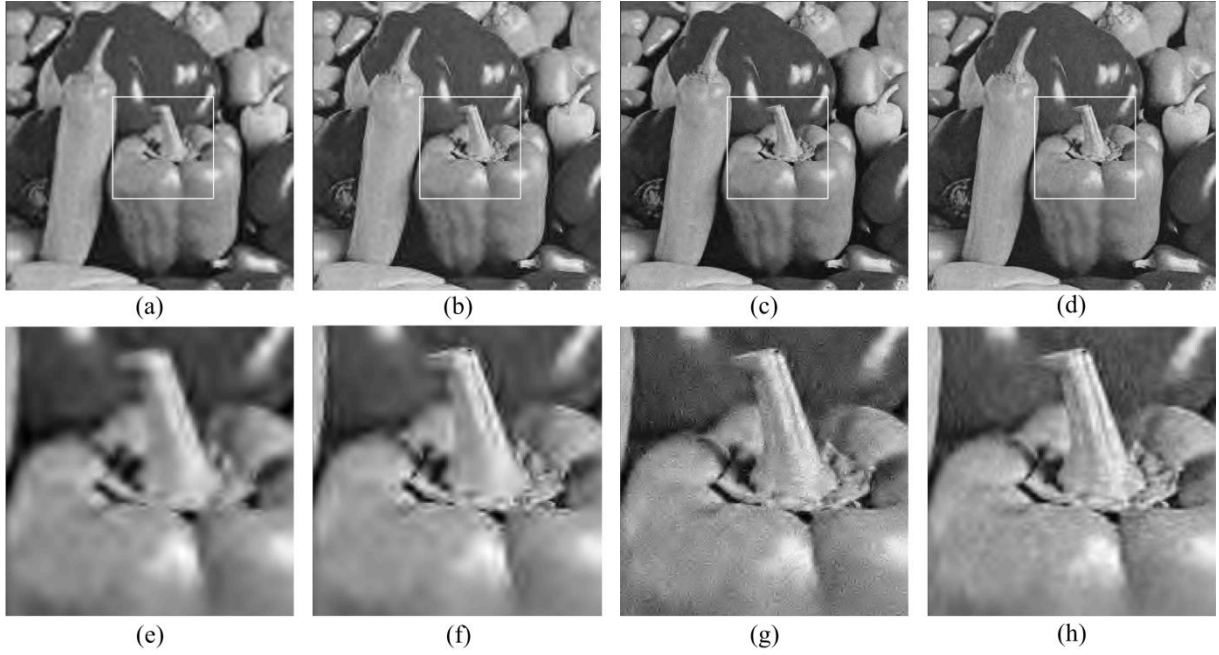


Fig. 8. The comparison of four methods on the 512×512 Peppers with $\sigma=20$. (a) soft thresholding (26.82dB), (b) hard thresholding (28.16dB), (c) neighshrink (28.88dB), (d) our method (29.94dB); (e), (f), (g), (h) are the zoomed local regions of (a), (b), (c), (d), respectively.

Table 2. PSNR values (dB) of the denoised images provided by four denoising methods.

Image size (pixel)	Noisy image(dB)		Soft thresholding		Hard thresholding		NeighShrink		Our method	
	512×512	256×256	512×512	256×256	512×512	256×256	512×512	256×256	512×512	256×256
Lena										
$\sigma=10$	28.12	28.12	29.10	25.82	30.98	27.75	33.10	31.17	33.51	31.01
$\sigma=15$	24.63	24.57	27.87	24.82	29.37	26.36	30.79	28.88	31.65	28.85
$\sigma=20$	22.13	22.15	27.10	24.13	28.30	25.28	29.11	27.27	30.38	27.41
$\sigma=25$	20.25	20.24	26.53	23.63	27.51	24.59	27.76	25.94	29.36	26.43
$\sigma=30$	18.72	18.68	26.10	23.34	26.82	24.14	26.57	24.85	28.40	25.72
Cameraman										
$\sigma=10$	28.29	28.26	29.58	25.26	32.07	27.70	34.12	31.21	35.21	30.99
$\sigma=15$	24.88	24.85	27.95	23.99	30.12	25.99	31.41	28.79	32.86	28.80
$\sigma=20$	22.44	22.40	26.84	23.12	28.73	24.82	29.31	27.05	31.22	27.27
$\sigma=25$	20.57	20.61	26.01	22.53	27.56	24.02	27.73	25.73	29.80	26.34
$\sigma=30$	19.02	19.05	25.34	21.95	26.74	23.21	26.33	24.45	28.75	25.28
Barbara										
$\sigma=10$	28.12	28.11	25.28	25.37	27.69	26.90	31.42	30.55	31.44	29.77
$\sigma=15$	24.60	24.59	24.06	24.53	25.51	25.63	28.95	28.44	29.04	27.92
$\sigma=20$	22.17	22.17	23.45	24.07	24.32	24.92	27.22	27.01	27.39	26.81
$\sigma=25$	20.24	20.24	23.13	23.72	23.65	24.46	25.82	25.83	25.88	25.81
$\sigma=30$	18.72	18.72	22.92	23.44	23.27	24.00	24.78	24.73	24.73	25.27
Peppers										
$\sigma=10$	28.26	28.16	28.88	26.86	30.68	29.17	32.76	32.15	32.82	32.20
$\sigma=15$	24.78	24.64	27.67	25.50	29.29	27.33	30.64	29.60	31.12	29.88
$\sigma=20$	22.32	22.23	26.82	24.64	28.16	26.25	28.88	27.87	29.94	28.34
$\sigma=25$	20.44	20.29	26.15	24.01	27.23	25.33	27.53	26.27	28.81	27.28
$\sigma=30$	18.91	18.78	25.66	23.54	26.51	24.61	26.33	25.11	27.92	26.40

As shown in Fig. 5, 6, 7, and 8, the proposed method gave the best denoised results. The denoised images provided by the soft thresholding and the hard thresholding were blurred seriously, especially for the edge regions (Fig. 6 (e) and (f)) and the texture regions (Fig. 7 (e) and (f)). Both the proposed method and the *NeighShrink* scheme preserved the edges and the textures of the images very well. The details of the images are well preserved by the *NeighShrink* scheme, but the noise removal introduced some artifacts. These artifacts result in a bad smoothness, which can be seen from the zoomed local regions of the denoised images (Fig. 5 (g), Fig. 6 (g), Fig. 7 (g) and Fig. 8 (g)). The denoised images indicate that the details (around the eyes of Lena), the textures (the knee of Barbara), the sharp edges (around the camera of Cameraman), and the smooth regions (Peppers) are well preserved by the proposed method without introducing too many artifacts.

According to Table 2, the output PSNRs of denoised images can be improved obviously by four methods. The results show that the proposed method outperforms the soft thresholding, the hard thresholding, and the *NeighShrink* scheme for all noise levels. The average gains of the proposed method are 3.68dB, 2.28dB, 0.61dB, respectively. Unlike the soft and hard thresholding, which set the small coefficients to zero, the proposed method adaptively changes the shrinkage functions to shrink the small coefficients. This is reason why the proposed method could give better gains than others.

INDIRECT COMPARISONS

In this part, the soft thresholding, the hard thresholding, and the proposed method are incorporated into the empirical wiener filtering and TI scheme for the denoising comparisons. These three methods are used in the first denoising process of the empirical wiener filtering and the shifted images' denoising of the TI scheme. The experimental results can reflect the efficiency of our method by applying it

to other denoising methods. For the empirical wiener filtering, the wavelet 'sym6' is used in the first wavelet transform and the wavelet 'sym8' is used in the second wavelet transform. Ten cyclic shifts are employed in the TI scheme. The denoised results in PSNR are listed in Table 3.

According to the denoised results, our method combined with the empirical wiener filtering and TI denoising produced the highest PSNR values (shown as bold fonts). It clarified that compared with the soft and hard thresholding, the proposed method is more effective when it is incorporated into other denoising methods.

CONCLUSIONS

A novel and effective image denoising algorithm which adaptively used different shrinkage functions to shrink different wavelet coefficients was researched in this paper. The number of the large coefficients, which neighbored with each small coefficient in an 11×11 neighborhood window, is employed to determine the shrinkage function. The denoising results show that the proposed method is superior to soft threshold method, hard threshold method and *NeighShrink* scheme in detail representation and numerical results after denoising. The PSNR values resulting from the proposed new method are higher than that of resulted from the soft and hard thresholding. Moreover, the new method can obtain a better result when the customized wavelets, the adaptive threshold, the special modeling, etc. are employed.

ACKNOWLEDGMENT

This work is financially supported by the National Natural Science Foundation of China (Grant No. 62174134) and Shaanxi Innovation Capability Support Project (Grant No. 2021TD-25).

Table 3. *PSNR values (dB) of the denoised images provided by the empirical wiener filtering and TI scheme with three denoising methods.*

Image size (pixel)	Noisy image (dB)		Wiener (soft thresholding)		Wiener (hard thresholding)		Wiener (our method)		TI (soft thresholding)		TI (hard thresholding)		TI (our method)	
	512×512	256×256	512×512	256×256	512×512	256×256	512×512	256×256	512×512	256×256	512×512	256×256	512×512	256×256
Lena														
$\sigma=10$	28.14	28.12	32.13	28.63	33.09	29.66	34.04	31.64	29.26	26.03	31.93	28.83	33.98	31.72
$\sigma=15$	24.62	24.63	30.46	27.03	31.58	28.17	32.25	29.32	28.02	24.91	30.20	27.09	32.10	29.37
$\sigma=20$	22.14	22.16	29.14	26.03	30.30	27.14	31.11	28.04	27.15	24.24	28.88	25.97	30.76	27.95
$\sigma=25$	20.25	20.25	28.27	25.34	29.34	26.27	30.15	27.05	26.63	23.72	28.07	25.12	29.78	26.94
$\sigma=30$	18.70	18.74	27.61	24.81	28.55	25.69	29.30	26.48	26.21	23.39	27.34	24.59	28.84	26.15
Cameraman														
$\sigma=10$	28.28	28.26	33.56	28.27	34.80	29.27	35.79	31.29	29.92	25.45	33.66	28.76	36.22	31.47
$\sigma=15$	24.87	24.87	31.64	26.63	32.65	27.57	33.50	29.24	28.21	24.08	31.35	26.90	33.66	29.29
$\sigma=20$	22.45	22.45	30.21	25.58	31.19	26.42	31.93	27.92	27.06	23.23	29.80	25.67	31.92	27.85
$\sigma=25$	20.53	20.54	28.89	24.56	29.87	25.48	30.56	26.64	26.13	22.56	28.46	24.65	30.39	26.56
$\sigma=30$	19.04	19.03	27.88	23.88	28.86	24.87	29.50	25.71	25.48	22.07	27.43	23.83	29.19	25.55
Barbara														
$\sigma=10$	28.13	28.15	27.65	27.51	29.11	28.43	32.03	30.07	25.42	25.53	28.80	27.72	32.50	30.27
$\sigma=15$	24.61	24.62	25.47	26.30	26.67	27.15	29.71	28.33	24.16	24.62	26.32	26.24	29.92	28.24
$\sigma=20$	22.14	22.19	24.38	25.57	25.15	26.31	27.96	27.23	23.53	24.14	24.84	25.43	28.04	27.05
$\sigma=25$	20.25	20.26	23.83	25.03	24.36	25.73	26.56	26.40	23.20	23.77	24.04	24.85	26.58	26.17
$\sigma=30$	18.71	18.73	23.50	24.57	23.83	25.19	25.20	25.74	22.99	23.49	23.53	24.38	25.17	25.50
Peppers														
$\sigma=10$	28.24	28.15	31.71	30.45	32.44	31.51	33.06	32.46	29.01	27.18	31.54	30.44	33.10	32.64
$\sigma=15$	24.76	24.62	30.27	28.43	31.09	29.54	31.44	30.17	27.78	25.63	30.06	28.29	31.41	30.25
$\sigma=20$	22.32	22.20	29.09	27.31	29.93	28.39	30.27	28.83	26.91	24.86	28.86	27.10	30.14	28.75
$\sigma=25$	20.45	20.32	28.13	26.20	28.93	27.37	29.30	27.95	26.27	24.16	27.83	25.99	29.04	27.76
$\sigma=30$	18.93	18.81	28.08	25.46	27.37	26.52	28.45	27.14	25.80	23.73	27.08	25.32	28.14	26.75

REFERENCES

- Alessandro M., Juan M. H., Mercedes E. P. et al. (2020). A Single Model CNN for Hyperspectral Image Denoising. *IEEE Trans. Geosci. Remote Sens.* 58(4):2516-29.
- Cai T. T., Silverman B. W. (2001). Incorporating information on neighboring coefficients into wavelet estimation. *Sankhya: Ind. J. Stat. B*, pt. 2 63:127-48.
- Çelik T., Özkaramanlı H., Demirel H. (2008). Facial feature extraction using complex dual-tree wavelet transform. *Comput. Vision Image Understanding* 111:229-46.
- Chang S.G., Yu B., Vetterli M. (2000). Spatially adaptive wavelet thresholding with context modeling for image denoising. *IEEE Trans. Image Process.* 9(9):1522-31.
- Chen G. Y., Bui T. D. (2003). Multiwavelets Denoising Using Neighboring Coefficients. *IEEE Signal Process Lett.* 10(7):211-14.
- Chen G.Y., Bui T.D., Krzyzak A. (2005). Image denoising with neighbour dependency and customized wavelet and threshold. *Pattern Recognit.* 38:115-24.
- Chen Y. and Han C. (2005). Adaptive wavelet threshold for image denoising. *Electron. Lett.* 41(10):586-87.
- Choi H., Baraniuk R.G. (1998). Analysis of Wavelet-Domain Wiener Filters. *the IEEE-SP Int. Sym. on Time-frequency and Time-scale Analysis* 613-16.
- Choi H., Baraniuk R.G. (2004). Multiple wavelet basis image denoising using Besov ball projections. *IEEE Signal Process Lett.* 11(9):717-20.
- Coifman R. R., Dohono D. L. (1995). Translation-invariant de-noising. in *Wavelets and Statistics*, A. Antoniadis and G. Oppenheim, Eds., New York, Springer-Verlag 125-50.
- Dohono D.L. (1995). De-noising by soft-thresholding. *IEEE Trans. Inf. Theory* 41(3):613-27.
- Dohono D.L., Johnstone I.M. (1994). Ideal spatial adaptation by wavelet shrinkage. *Biometrika* 81(3):425-55.
- Dohono D.L., Johnstone I.M. (1995). Adapting to unknown smoothness via wavelet shrinkage. *J. Amer. Statist. Assoc.* 90:1200-24.
- Fadi B., Naser D., Florian K., Arjan K. (2022). Self-restrained triplet loss for accurate masked face recognition. *Pattern Recognit.* 124:108473.
- Ghael S., Sayeed A., Baraniuk R. (1997). Improved wavelet denoising via empirical wiener filtering. *Proc. SPIE, San Diego* 3169:389-99.
- Gonzalez R.C., Woods R.E. (2002). *Digital Image Processing*. 2nd ed. Prentice-Hall, Englewood CliffsNew Jersey,
- Lalith K. S. S., Otto M., Irène B., Luc B., Thomas B. (2021). Potentials and caveats of AI in hybrid imaging. *Methods*, 188:4-19.
- Mallat S. (1989). A theory for multiresolution signal decomposition: The wavelet representation. *IEEE Trans. Pattern Anal. Machine Intell.* 11:674-93.
- Sendur L., Selesnick I.W. (2002a). Bivariate shrinkage functions for wavelet-based denoising exploiting interscale dependency. *IEEE Trans. Signal Process.* 50(11):2744-56.
- Sendur L., Selesnick I. W. (2002b). Bivariate Shrinkage with Local Variance Estimation. *IEEE Signal Process Lett.* 9(12):438-41.
- Shengqian W., Yuanhua Z., Daowen Z. (2002). Adaptive shrinkage de-noising using neighborhood characteristic. *Electron. Lett.* 38(17):502-3.
- Simoncelli E.P., Adelson E.H. (1996). Noise removal via Bayesian wavelet coring. *The 3rd Int. Conf. on Image Process., Lausanne, Switzerland* 1:379-82.
- Ying Y., Yusen W. (2010). Random Interpolation Average for Signal Denoising. *Signal Process., IET.* 4(6):708-19.
- Ying Y., Yusen W. (2013). Random interpolation average for ECG signal denoising using multiple wavelet bases. *Biomed. Eng. Appl. Basis Commun.* 25(4), 1350042.
- Yu-Hsuan H., Homer H. C. (2022). Deep face recognition for dim images. *Pattern Recognit.* 126:108580.
- Zhou D., Cheng W. (2008). Image denoising with an optimal threshold and neighbouring window. *Pattern Recognit. Lett.* 29:1694-97.